Thi_Qar University Journal for Engineering Sciences
http://www.doi.org/10.31663/tqujes.9.2.326(2018)
Vol.9 No.2 (September 2018)
ISSN 2075-9764
Available at http://jeng.utq.edu.iq
engjrnal@jeng.utq.edu.iq

Theoretical Study of the Effect of Water Basin Shape on Productivity of Tubular Solar Still

Wisam A. Abd Al-wahid†

† Engineering Technical College/Najaf, Al-Furat Al-Awasat Technical University, 31001 Al-Najaf, Iraq.

Abstract

Present work, studies effect of basin shape on productivity of tubular solar still (TSS). Basin works as solar energy absorber to transfer this energy to saline water by diffusion (conduction and convection). After absorbing the energy, water transforms into vapor to condensate on the outer cover of TSS. In present work, shape of the basin modified into four cases taken here to increase solar energy absorption and inside water convection. This led to increase the productivity of fresh water to reach maximum value of 47% than regular basin. This is a passive method of modification of water productivity, which applied easily in practical applications.

Keywords: sustainable energy, fresh water productivity, tubular solar still.

1. Introduction

In natural circle of water, it evaporated from its sources (lakes, oceans, seas, rivers, etc), accumulate as clouds and return as rains or snow after condensation due to decrease in temperature. This circle gave us the necessary fresh water of life for millions of years. In recent years, after the appearance of water sources pollution and lack of fresh water in the price of salinity water increment, reproduction of that natural circle (on a small range) is one of the brilliant ideas human mind came with to produce a water with no pollutants and acceptable PH scale. The idea is to use solar energy as motivation energy in that process, where no pollution or side effects found. Regardless of high cost of the structure, solar energy is cheap and available around the year especially in countries suffering from dryness.

Researchers, encouraged by companies and high need of new water resources, developed this process and took in mind the variables in it, in order to have highest productivity. Some researchers reviewed the literatures in the field and presented the works in two shapes, the experimental developments [1], and the theoretical field [2].

Since the solar energy is the engine in the process, the non-uniformity of the solar flux cause structure problems [3, and 4]. The solution of the problem is by good mix of the working fluid (saline water) to decrease the temperature difference. In the other hand, the productivity was the main aim of the studies. Therefore, evaluating of the heat transfer coefficient took the attention in order to have larger efficiency by knowing the affecting parameters [5, and 6], by changing the compound shape [7, and 8], or by studying the parameters for a certain place [5], or to different operational conditions [9]. Vacuum pressure was one of the parameters studied [11], or the combination of multi stages [5, and 10].

Literatures took the two methods of work, experimental [1, 8, 10, and 11], or theoretical [2, 3, 4, 5, 6, 7, and 9], but the CFD simulation show to be a good tool to investigate the heat transfer coefficients and productivity [6]. Therefore, in present work, numerical simulation of effect of the water basin shape, with different arrangements done to enhance the efficiency of heat transfer since saline water temperature has the greater effect on the productivity [4], where an arrangements as that shown in figure 1, may augment the efficiency. Another variable took is the depth of saline water and investigate the effect of this variable on water productivity.

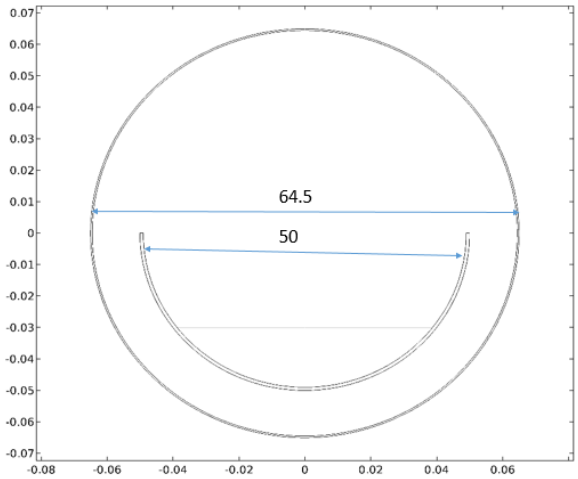

(a) Case 1.

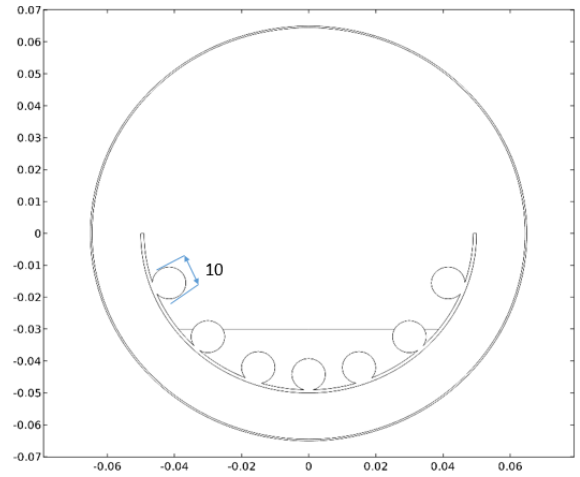

(b) Case 2.

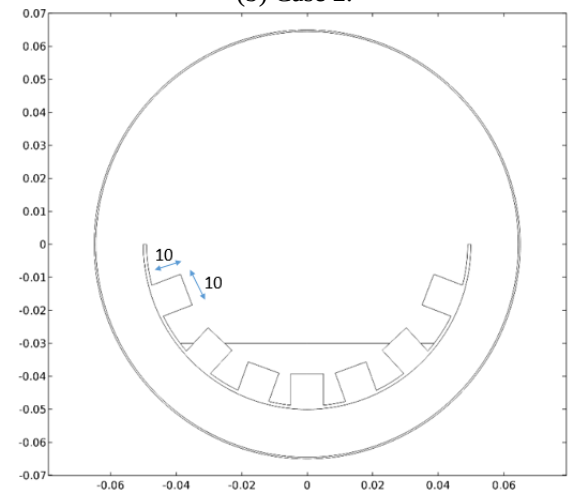

(c) Case 3.

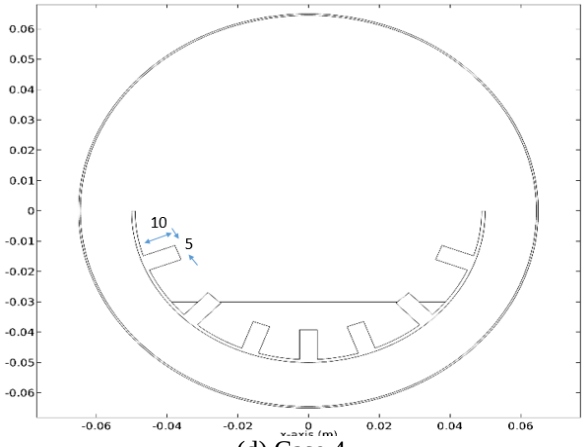

(d) Case 4.

Figure 1 (a) Regular tubular solar still, (b, c and d) modified water basin shapes (dimensions are in mm).

2. Mathematical model:

Figure 2 below, shows heat transfer modes in inside and outside of TSS. These kinds of heat transfers related to the processes occurring there, which are:

1- Evaporation of water into vapor Q1.
2- Heat exchange between saline water surface and vapor by convection Q2.
3- Heat transfer from vapor to trough by convection Q3.
4- Heat transfer between trough and saline water Q4.
5- Heat transfer between vapor and TSS cover Q5.
6- Heat transfer from TSS cover into ambient Q6.
7- Condensation process on TSS cover from inside Q7.
8- Radiation exchange between saline water surface and TSS cover Q8.
9- Radiation exchange between TSS cover to ambient Q9.

Besides the radiations of Solar (Rs) which is absorbed by:

1- Saline water Rw.
2- TSS cover Rc.
3- Trough Rt.
4- Vapor Rha

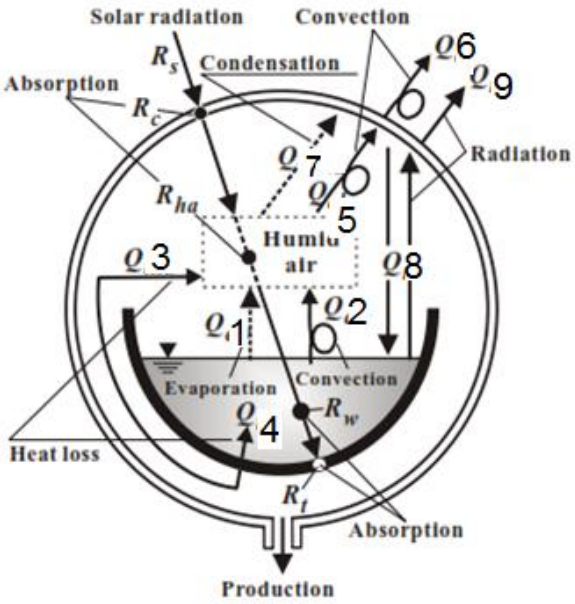

Fig.2 Heat modes inside and outside of (TSS).

2.1 Equations of energy balance:

Energy balance of TSS parts expressed as follows [12]:

a) TSS cover:

$$(\rho C_p V)_c \frac{\partial T_c}{\partial t} = R_c + Q_5 + Q_7 + Q_8 - Q_6 - Q_9 \quad (1)$$

Where:

$$R_c = \tau_c . R_s . d . l_c \quad (2)$$

$$\tau_c = (1 - al_c)\alpha_c \quad (3)$$

$$Q_5 = h_5(T_{ha} - T_c)A_c \quad (4)$$

$$Q_7 = h_{lv}h_7(\rho_{vha} - \rho_{vc})A_c \quad (5)$$

$$Q_8 = h_8(T_w - T_c)A_w \quad (6)$$

$$Q_6 = h_6(T_c - T_a)A_c \quad (7)$$

$$Q_9 = h_9(T_c - T_a)A_c \quad (8)$$

b) Vapor:

$$(\rho C_p V)_{ha} \frac{\partial T_{ha}}{\partial t} = R_{ha} + Q_1 + Q_2 + Q_3 - Q_5 - Q_7 \quad (9)$$

Where:

$$R_{ha} = \tau_{ha} . R_s . A_{ha} \quad (10)$$

$$\tau_{ha} = (1 - al_c)(1 - \alpha_c)\alpha_{ha} \quad (11)$$

$$Q_1 = h_{lv}h_1(\rho_{vw} - \rho_{vha})A_w \quad (12)$$

$$Q_2 = h_2(T_w - T_{ha})A_w \quad (13)$$

$$Q_3 = h_3(T_t - T_{ha})A_3 \quad (14)$$

Q5 and Q7 from eq. (4), (5).

c) Saline water [12]:

$$(\rho C_p V)_w \frac{\partial T_w}{\partial t} = R_w + Q_4 - Q_1 - Q_2 - Q_8 \quad (15)$$

Where:

$$R_w = \tau_w R_s A_w \quad (16)$$

$$\tau_w = (1 - al_c)(1 - \alpha_c)(1 - \alpha_{ha})(1 - al_w)\alpha_w \quad (17)$$

$$Q_4 = h_4(T_t - T_w)A_4 \quad (18)$$

Q1, Q2, and Q8 from eq. (12), (13), (6), respectively.

d) TSS:

$$(\rho C_p V)_t \frac{\partial T_t}{\partial t} = R_t - Q_4 - Q_3 \quad (19)$$

Where:

$$R_t = \tau_{t1} R_s A_w + \tau_{t2} R_s (B_t l_t - A_w) \quad (20)$$

$$\tau_{t1} = (1 - al_c)(1 - \alpha_c)(1 - \alpha_{ha})(1 - al_w)(1 - \alpha_w)(1 - al_t)\,\alpha_t \quad (21)$$

$$\tau_{t2} = (1 - al_c)(1 - \alpha_c)(1 - \alpha_{ha})(1 - al_t)\,\alpha_t \quad (22)$$

Q4 and Q3 from eqs. (18), (14).

2.2 Mass and Heat transfer coefficients:

1) Coefficients of Mass transfer:

a) Coefficient of Mass transfer in Evaporation:

Heat fluxes due water evaporation given by product of evaporation heat (hlv) and vapor mass flux:

$$Q_1 = h_{lv}h_1(\rho_{vw} - \rho_{vha}) \quad (23)$$

Where, h1 is evaporation coefficient of mass transfer between water surfaces and vapor:

$$h_1 = 5.86 * 10^{-3} + 6.5 * 10^{-5}(T_w - T_c) \quad (24)$$

b) Condensation mass transfer coefficient:

Condensation latent heat on TSS cover in the inner surface resulted from product of hfg and condensation mass flux, as below [9]:

$$Q_7 = h_{fg}h_7(\rho_{vha} - \rho_{vc}) \quad (25)$$

Where, h7 is coefficient of condensation mass transfer of vapor that is:

$$h_7 = 1.55 * 10^{-3} + 1.97 * 10^{-5}(T_w - T_c) \quad (26)$$

2) Coefficients of Heat transfer:

a) Convection heat transfer coefficient:

i) Convection heat (Q2) between water and vapor given by cooling law of Newton [9]:

$$Q_2 = h_2(T_w - T_{ha}) \quad (27)$$

Where, h2 is convection heat coefficient between water and vapor expressed as:

$$h_2 = 25.32 * 10^{-2} + 13.11 * 10^{-2}(T_w - T_c) \quad (28)$$

ii) Convective heat transfer between vapor and cover given by:

$$Q_5 = h_5(T_{ha} - T_c) \quad (28)$$

Where, h5 is convection coefficient between vapor and TSS cover, given by:

$$h_5 = -3.35 * 10^{-2} + 4.04 * 10^{-2}(T_w - T_c) \quad (29)$$

iii) Heat transfer by convection between cover and ambient calculated by the following equation:

$$Q_6 = h_6(T_c - T_a) \quad (30)$$

Where, h6 is convection heat coefficient between TSS cover and ambient, and:

$$h_6 = 5.7 + 3.8 * Ve \quad (31)$$

b) Radiation heat coefficient:

i) Radiation heat coefficient in TSS calculate by [12]:

$$Q_8 = h_8(T_w - T_c) \quad (32)$$

Where, h8 is radiation heat coefficient between saline water surface and TSS cover, which is:

$$h_8 = \frac{\sigma(T_w^2 + T_c^2)(T_w + T_c)}{\frac{1}{\epsilon_w} + (\frac{1}{\epsilon_c} - 1)\frac{A_w}{A_c}} \quad (33)$$

ii) Radiation heat transfer between TSS cover and ambient (Q9) given by:

$$Q_9 = h_9(T_c - T_a) \quad (34)$$

Where, h9 is:

$$h_9 = \frac{\sigma(\epsilon_c T_c^4 - \epsilon_{sky} T_{ambient}^4)}{(T_c - T_a)} \quad (35)$$

$$T_{sky} = 137.5 + 0.5 * T_a \quad (36)$$

2.3. Governing Equations of vapor:

Flow of vapor and energy transfer based on fundamental governing equations of fluid dynamics, continuity in two dimensions, momentum in two dimensions, energy diffusion, and mass concentration equations of vapor as following:

1- Continuity Equation:

Equation for mass conservation applied to air mixture as carrying fluid is:

$$\frac{\partial \rho}{\partial t} + \frac{\partial u}{\partial x}\rho + u\frac{\partial \rho}{\partial x} + \frac{\partial u}{\partial y}\rho + v\frac{\partial \rho}{\partial y} = 0 \quad (37)$$

2- Conservation of Momentum Equations:

(i) Horizontal momentum equation:

$$u\frac{\partial u}{\partial x} + v\frac{\partial u}{\partial y} = -\frac{1}{\rho}\frac{\partial P}{\partial x} + \upsilon\left(\frac{\partial^2 u}{\partial x^2} + \frac{\partial^2 u}{\partial y^2}\right) \quad (38)$$

(ii) Vertical momentum eqation:

$$u\frac{\partial v}{\partial x} + v\frac{\partial v}{\partial y} = -\frac{1}{\rho}\frac{\partial P}{\partial y} + \upsilon\left(\frac{\partial^2 v}{\partial x^2} + \frac{\partial^2 v}{\partial y^2}\right) + F \quad (39)$$

$$F = g[\beta_T(T - T_c) + \beta_s(c - c_c)] \quad (40)$$

2.4 Energy Conservation Equation:

1. **Equation of conservation of energy given by**:

$$u\frac{\partial T}{\partial x} + v\frac{\partial T}{\partial y} = \alpha\left(\frac{\partial^2 T}{\partial x^2} + \frac{\partial^2 T}{\partial y^2}\right) \quad (41)$$

4- Concentration Equations:

$$u\frac{\partial C}{\partial x} + v\frac{\partial C}{\partial y} = D_{AB}\left(\frac{\partial^2 C}{\partial x^2} + \frac{\partial^2 C}{\partial y^2}\right) \quad (42)$$

2.4 Boundary conditions of moist air:

Boundary conditions are as following;

i) Inner glass cover: u=0, v=0, T=Tc, c=Cc|T=Tc, Φ=100%

Where:

$$C_c = P_{sat}/(R.T_c) \quad (43)$$

ii) Water surface: u=0, v=0, T=Tw, c=Cw|T=Tw, Φ=100%

Where:

$$C_w = P_{sat}/(R.T_w) \quad (44)$$

iii) Trough walls: u=0, v=0,

$$\frac{\partial T}{\partial x} = 0 \, , \frac{\partial c}{\partial x} = 0$$

3. Numerical procedure:

Numerical procedure divided into two parts;

First Part: - by using above energy balances equations where they solved numerically by using computer software (v5.3 of COMSOL Multiphysics software) to find surface temperature of saline water Tw, vapor Tha, and trough Tt and TSS cover Tc. These calculations are function of solar radiation, ambient temperature, and wind velocity. All these values introduced depending on conditions of Najaf city in Iraq. The previous values used as initial calculations in which software calculates mentioned variables. Radiation energy and ambient temperature values taken from experimental data of literatures, and depend on energy balance equations.

second part: - After applying computations of first part, solution of governing equations (37), (38), (39),

(40), (41), and (42) for vapor to predict temperatures distribution inside TSS, concentration of vapor, flow streamline inside TSS, and productivity.

The solution of the differential equations done numerically by using COMSOL Multiphysics 5.2, where finite volume procedure used. Meshing generation and refinement of system very important to find heat fluxes and fluid motion in complex geometries. Therefore, both mesh density and lines distribution play important roles in accuracy. In solution of problem, flow assumed two-dimensional, unsteady, and laminar.

The number of elements used according to grid dependency where results settled is about 13720 elements.

The first step is to validate results obtained here with that of literatures. The experimental work of [12], as well as numerical results of [9] used to validate numerical solution as shown in figure 3 below.

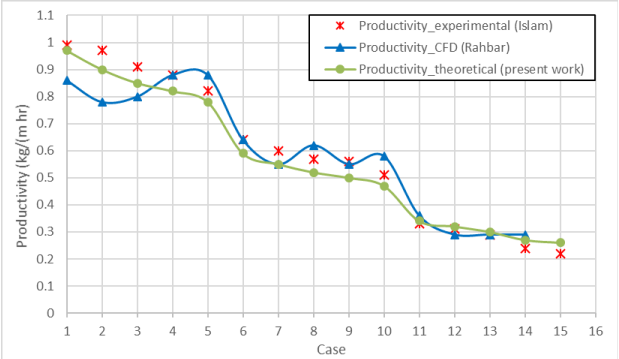

Figure 3 Validation of present work with [12] and [9].

The figure shows a good agreement with both results, which considered as a hint of validity of results obtained here.

4. **Results and discussions**:

Results obtained by numerical calculation presented here. Four cases taken to study the effect of basin shape modification. For reasons of comparison, similar saline water depth taken for each study, since this depth is one of the effective characters affecting productivity (as will be shown later). In present work, three values of saline water depths taken, 10mm, 15mm, and 20mm. Another characters fixed in the aim of comparison are solar energy (800 W/m2) and ambient temperature (35 oC), where they changed during daytime.

Figures 4, 5, 6, and 7 show the concentration of water's vapor contour for cases 1, 2, 3, and 4 respectively. For standard case, vapor concentration takes its extreme value near the surface of saline water. Vapor rise vertically, concentrated at the middle of the tubular solar still, according to buoyance effect. Vapor hits the top of the glass cover and spread in the shape of two symmetric eddies. By comparing with other modified cases, same behavior obtained for each case. In the other hand, comparison shows an increment of vapor concentrations values especially for case 2 (figure 5), where 21% increment than regular case appeared. Case 3 shows an increment about 15% (figure 6), while case 4 (figure 7) shows 12% increment. The increment regarded to increase in ability of solar radiation absorption due to increase in radiation shape factor. This increment led to rise of energy transported into saline water, where more water molecules get their latent heat and vaporized.

Figures 8, 9, 10, and 11 show streamline of vapor flow for cases 1, 2, 3, and 4 respectively. As expected due to vapor motion shown latterly, big twin eddied shown to cover most of the space of tubular solar still. These eddies are symmetric around vertical axis. The comparison of case 2 (figure 9) with regular case (figure 8), shows more violent motion of the big eddies due to increase in streamlines velocities. This increment shown less by comparing with case 3 (figure 10).

Figures 12, 13, 14, and 15 show temperature distribution of water vapor in cavity area of tubular solar still. In figure 12, isotherms lines shown to be semi-flat lines as departed from water surface. As lines rise its temperature decrease gradually. The lines lost their flatness in the middle area as they go up until showing dramatic rise due to high velocity of vapor. In eddies area, temperature difference shown to be less than that near water surface. In the modified basins, isotherms show parallel, but not flat, lines decreased in their values as rising up from water surface. Case 2 (figure 13) appears to have higher values of isotherms values than other cases. Other modified basins (figure 14 and 15) also show an increment, but less than case 2, compared to original case.

Figures 16 and 17, show mean temperature values of saline water and glass cover respectively. In these figures, each case studied with different saline water depths in order to investigate the effect of this variable. Figures shown an increment due to modifications in both saline water and glass covers temperatures with a parallel behavior. Where any increment in saline water temperatures shows same amount of increment in glass cover temperature. This is a logical result of energy conservation laws. Saline water depths show an indirect effect on general process, where low depths show higher values of temperatures, which they decreased as water depths increased.

The most important character investigated is the productivity of fresh water. The cases compared with case 1 of classical basin to study increment or decrement of fresh water produced. Figure 18 shows values of productivity for each case with different depths. Case 2 shown to be most effective modification on productivity, since it produced ultimate values of fresh water. The increment is about 45% in 10 mm depth, 44% in 15 mm depth, and 47% in depth 20 mm. Cases 3 also show a significant increment of productivity values but they are less than that of case 2. The increments are 37% in 10 mm depth, 46% in 15 mm depth, and 46% in 20 mm depth. Case 4 shown to have the least increment for depths 20 mm (25 % of increment) and 15 mm (22 % of increment), with a negative effect in depth 10 mm (6% of decrement).

Modifications of basin shown to have an effect on the work of tubular solar stills. This effect shown to be a function of saline water depth as well as the kind of modification itself.

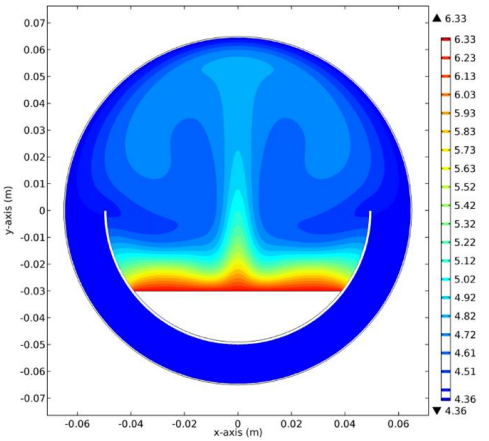

Figure 4 Vapor concentration for case 1.

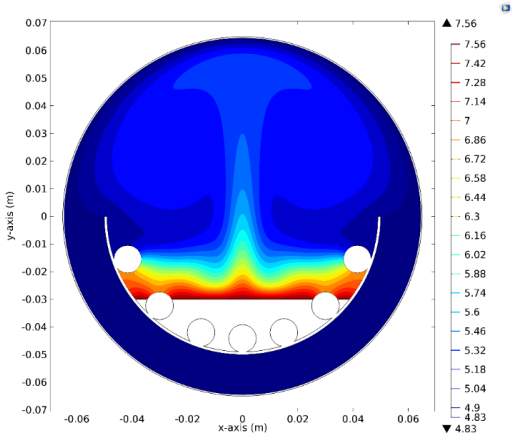

Figure 5 Vapor concentration for case 2.

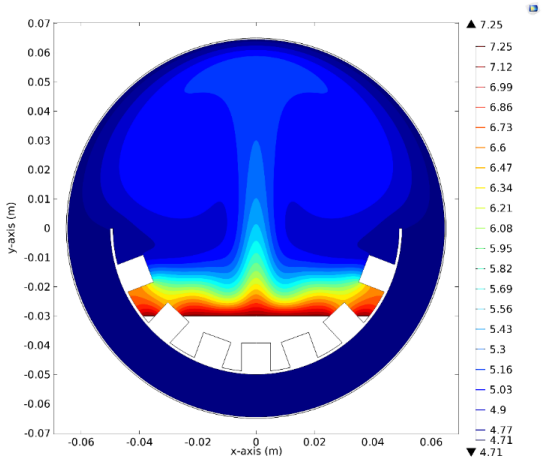

Figure 6 Vapor concentration for case 3.

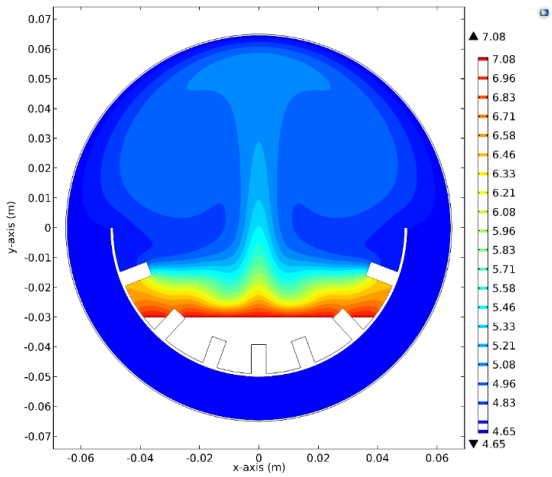

Figure 7 Vapor concentration for case 4.

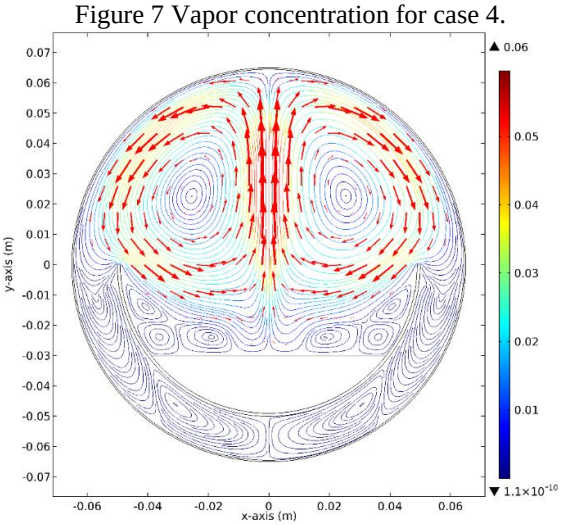

Figure 8 Streamlines of case 1.

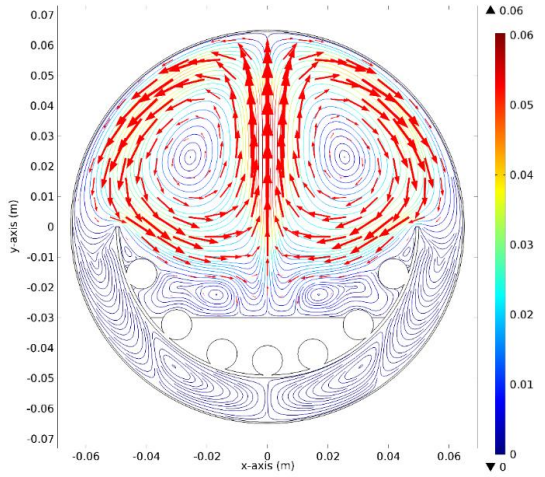

Figure 9 Streamlines of case 2.

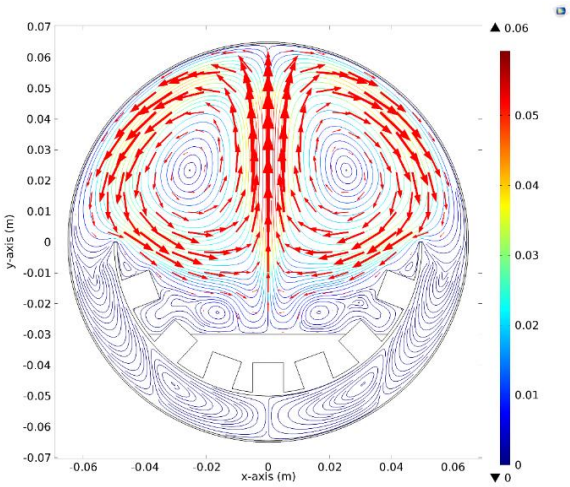

Figure 10 Streamlines of case 3.

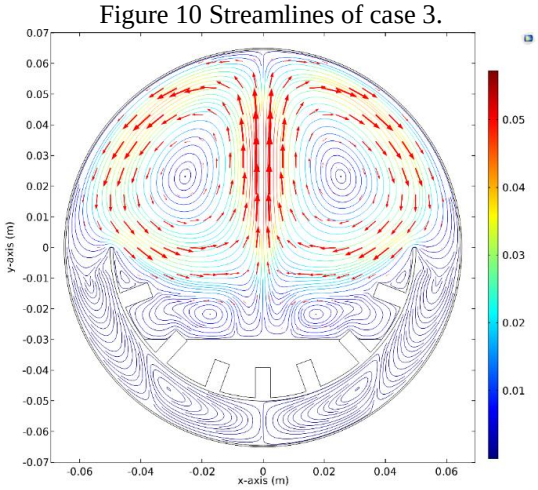

Figure 11 Streamlines of case 4.

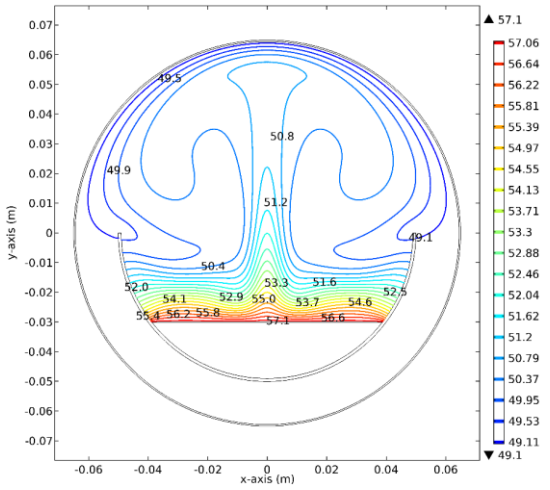

Figure 12 Temperature distribution for case 1.

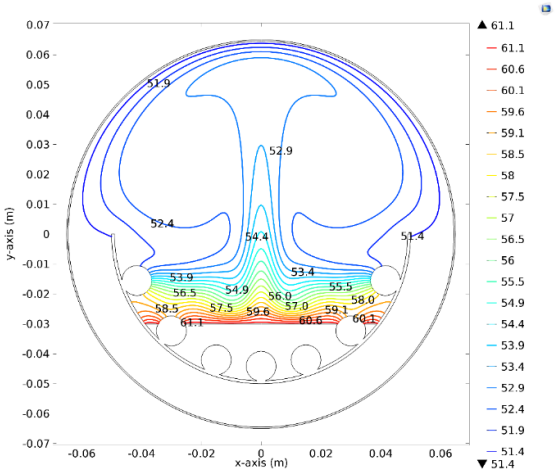

Figure 13 Temperature distribution of case 2.

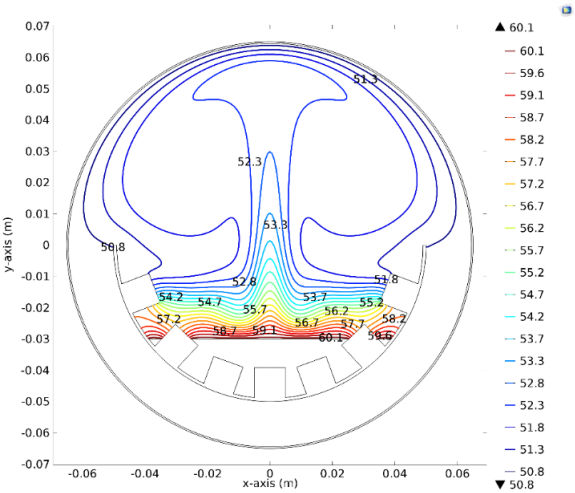

Figure 14 Temperature distribution of case 3.

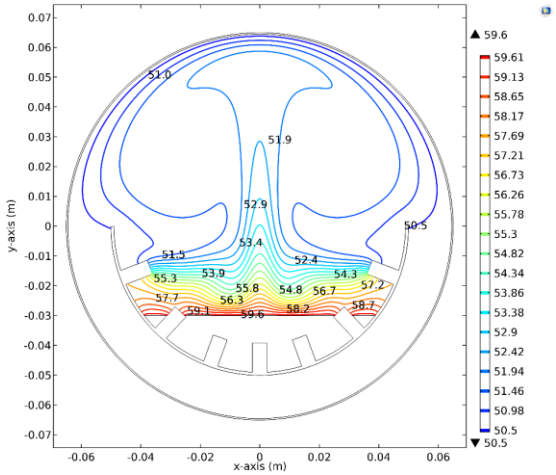

Figure 15 Temperature distribution of case 4.

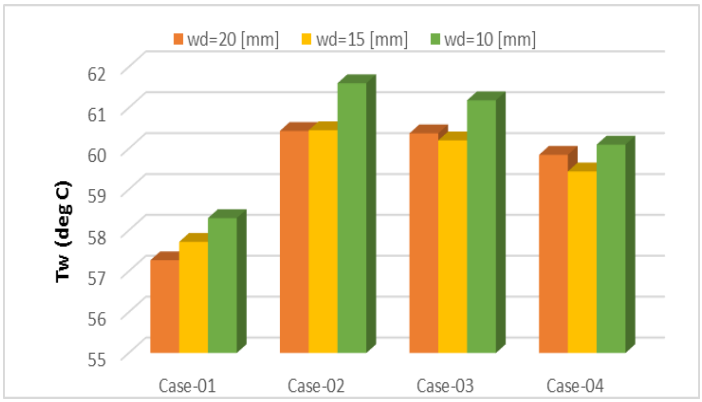

Figure 16 Saline water temperature at three water depths for each case.

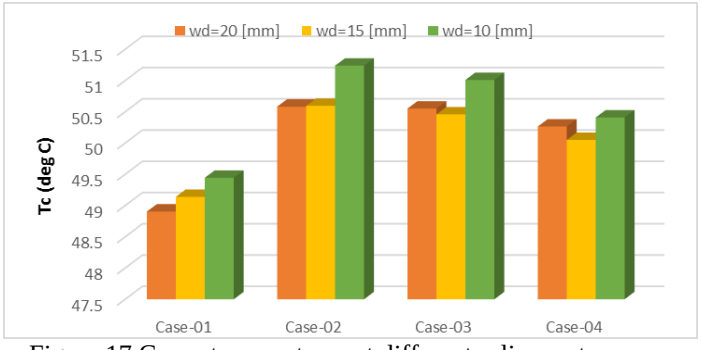

Figure 17 Cover temperatures at different saline water depths for each case.

5. Conclusions:

A modification on the shape of basins of tubular water still is applied. The change in the shape of the basin causes to increase shape factor to absorb solar radiation. This increment led to increase saline water temperature in the basin, which led to increase vapor concentrations. This cause to increase productivity of fresh water, which is the main factor to judge the benefits of using such modifications. Not all modifications led to positive productivity, where in one case (case 4) and certain water depth (10 mm), a negative productivity appeared.

Saline water depth in basins shown to have great effect on the whole process of productivity where it shown to be an important parameter. Indirect relation between water productivity and water depth.

Present work shown a passive method to increase productivity in tubular solar stills, which applied easily with great benefits.

6. References:

1- Rufuss, D. Dsilva, et. al., "Solar still: a comprehensive review of designs, performance and material advances", Renewable and Substantial Energy Reviews, No. 63, pp. 464-496, 2016.

2- Edalatpour, M., et al. "Solar stills: A review of the latest developments in numerical simulations", Solae Energy, 2016, http://dx.doi.org/10.1016/j.solener.2016.03.005.

3- Wei M, et al., "Design and optimization of baffled fluid distributor for realizing target flow distribution in a tubular solar receiver", Energy (2016), http://dx.doi.org/10.1016/j.energy.2016.04.0016.

4- Wei M, et al., "Fluid flow distribution optimization for minimizing the peak temperature of a tubular solar receiver", Energy, No. 91, pp. 663-677, 2015.

5- Bait, Omar, and Si-Ameur, Mohamed, "Numerical investigation of a multi-stage solar still under Benta climatic conditions: Effect of radiation term on mass and heat energy balances", Energy, No. 98, pp. 308-323, 2016.

6- Setoodeh, Narjes, et al., "Modelling and determination of heat transfer coefficient in a basin solar still using CFD", Desalination, No. 268, pp. 103-110, 2011.

7- Rashidi, S., et al., "Optimization of partitioning a single slope still for performance improvement", Desalination, No. 395, pp. 79-91, 2016.

8- Arunkumar, T., et al., "Productivity enhancement of comound parabolic concentrator tubular solar stills", Renewable Energy, No. 88, pp. 391-400, 2016.

9- Rahbar, Nader, et al., "Estimation of convective heat transfer coefficient and water-productivity in a tubular solar still-CFD simulation and theoretical analysis", Solar Energy, No. 113, pp. 313-323, 2015.
10- Xie, Guo, et al., "Conceptual design and experimental investigation involving a modular desalination system composed of arrayed tubular solar still", Applied Energy, pp. 972-984, 2016.
11- Wang, Pin-Yang, et al., "High temperature collecting performance of a new all-glass evacuated tubular solar air heater with U-shaped tube heat exchanger", Energy Conversion and Management, pp. 315-323, 2014.
12- Islam, K., Fukuhara, T. "Production analysis of a Tubular solar still", Doboku Gakkai Ronbunshuu B 63, P. 108-119, 2007.

Nomenclatures

Symbol	Description	Units
c	Vapor concentration of air	kg/m^3
DAB	Mass diffusivity of vapor	m/s
F	Buoyancy force	N/m^3
g	Gravitational acceleration (9.807)	m/s^2
h	Convection heat transfer coefficient	W/m^2K
Q	Heat amount	kJ/kg
R	Solar radiation	W
T	Temperature	K
u	Velocity in x-axis	m/s
v	Velocity in y-axis	m/s

Greek symbols

α	thermal diffusivity of air	m^2/s
βT	Volume expansion coefficient	1/K
βs	Species expansion coefficient	m^3/kg
μ	Viscosity	kg/m.s
ρ	Density	kg/m^3
ε	Emissivity	-
τ	Transmissivity	-